

Orbital excitation in Sr₂CuO₂Cl₂: Resonant inelastic x-ray scattering at the Cu *K* pre-edgeJungho Kim,^{1,2} D. S. Ellis,² T. Gog,¹ D. Casa,¹ and Young-June Kim^{2,*}¹*XOR, Advanced Photon Source, Argonne National Laboratory, Argonne, Illinois 60439, USA*²*Department of Physics, University of Toronto, Toronto, Ontario, Canada M5S 1A7*

(Received 3 November 2009; revised manuscript received 22 January 2010; published 25 February 2010)

We report resonant inelastic x-ray scattering (RIXS) study of *d-d* orbital excitations in Sr₂CuO₂Cl₂ utilizing the intermediate state associated with a quadrupole transition. Fourfold azimuthal angle dependence of the pre-edge peak near the Cu *K* absorption edge confirms that the in-plane pre-edge peak arises from the $1s \rightarrow 3d_{x^2-y^2}$ electric quadrupole transition. When the incident photon energy is tuned to this transition, we observed a RIXS excitation at 2 eV energy loss. This excitation is associated with the *d-d* excitation of $d_{x^2-y^2} \rightarrow d_{yz,zx}$ based on the angular dependence of the quadrupole transition-matrix element of the scattered photon.

DOI: 10.1103/PhysRevB.81.073109

PACS number(s): 78.70.Ck, 78.70.Dm, 71.70.Ch

Orbital excitations such as *d-d* excitations in transition-metal oxides have attracted much attention due to its fundamental importance in elucidating electronic structure. However, experimental study of these excitations between the crystal-field split *d* levels is difficult, since direct optical transition is dipole forbidden. Instead one has to rely on second-order processes such as Raman scattering¹ or nonlinear spectroscopy.² In recent years, the *d-d* excitations in cuprates have been investigated with resonant inelastic x-ray scattering (RIXS),³⁻⁸ which is a powerful photon-in photon-out probe of particle-hole excitations.⁹ In particular, RIXS in the soft x-ray regime such as Cu *M*_{2,3} (Ref. 3) and *L*₃ edges⁴ is an excellent tool for this purpose, since the intermediate states consist of 3*d* electron and a hole in either 3*p* or 2*p* states, respectively. These studies have shown that clear *d-d* excitations exist below 2 eV.^{3,4}

Recently, Larson *et al.*¹⁰ were able to use nonresonant inelastic x-ray scattering (NIXS) in the hard x-ray regime to observe *d-d* excitations in NiO and CoO. They showed that the NIXS cross-section of *d-d* excitation is enhanced significantly at large momentum transfer and is highly anisotropic in reciprocal space, reflecting the symmetry of the excitation. Despite its many advantages such as bulk sensitivity, hard x-ray NIXS suffers from small cross-section, especially for highly absorbing compounds such as cuprates. For example, in our preliminary NIXS measurements, *d-d* excitations in CuGeO₃ were observed with a count rate of ~ 7 counts per second, which is roughly an order of magnitude smaller than the charge-transfer (CT) excitation at 6.5 eV. Likewise, typical RIXS at the Cu *K* edge ($\underline{1s-4p}$, where underline denotes hole) also has a small cross-section for local *d-d* excitations,⁶ while the cross-section for charge-transfer excitations could be quite large.⁸

In this Brief Report, we show that RIXS in the hard x-ray range utilizing the seldom-used Cu $\underline{1s-3d}$ resonance, which can be reached via electric quadrupole (E2) transition, provides a complementary means for studying *d-d* excitations in cuprates. Similar studies at respective pre-edges have been carried out on Li₂CuO₂ (Ref. 5) and NiO.¹¹ Since a quadrupole transition is sensitive to the symmetry of the orbitals involved, considerable information on the symmetry of a *d-d* excitation can be gained by exploiting this resonance.

The $\underline{1s-3d}$ transition, which would occur in the pre-edge

energy range, just below the *K* absorption edge of Cu, is dipole forbidden and quadrupole allowed. Static or dynamic local distortion often relaxes the dipole selection rule, and allows such a pre-edge absorption structure to be observed. However, the perfect tetragonal D_{4h} symmetry of Sr₂CuO₂Cl₂ ensures that the observed $\underline{1s-3d}$ transition is almost entirely through the E2 channel. Our comprehensive angle-resolved x-ray absorption spectroscopy (XAS) experiment demonstrates the quadrupole nature of the absorption. Utilizing the intermediate states accessed through this E2 transition, we have carried out RIXS investigation of *d-d* excitations in this compound. Our RIXS spectra exhibit a broad excitation centered at 2 eV, whose scattered angle dependence agrees with the calculated angular dependence of the E2 matrix element for the $d_{x^2-y^2} \rightarrow d_{yz,zx}$ transition.

All measurements were carried out at the Advanced Photon Source 9IDB. The Si (333) reflection was used for the main monochromator. The sample was mounted on a six-circle diffractometer at room temperature in ambient condition for XAS, which was measured by monitoring total fluorescence yield using a solid-state detector. For RIXS measurements, additional spherically focusing (1 m radius of curvature) diced Ge(733) analyzer was added to resolve outgoing photon energy. The total-energy resolution for this RIXS setup using a point detector is about 300 meV (full width at half maximum, FWHM). For higher resolution RIXS measurements, the sample was cooled down (*T*=25 K) and additional Si(444) monochromator and position sensitive multistrip detector were used to provide total-energy resolution of 200 meV. The Sr₂CuO₂Cl₂ crystal was grown using the flux method as reported in Ref. 12.

Figure 1(a) shows the XAS data obtained with the photon polarization in the copper oxygen plane. All spectra were obtained with the photon momentum fixed at about 10° away from the copper-oxygen plane. In addition to the feature around 8995 eV due to the $\underline{1s-4p}$ dipole transition, there exists a small feature in the pre-edge region of 8979 eV. Since the E2 operator transforms as a spherical tensor of rank 2 and is sensitive to the symmetry of the final state, one can distinguish the quadrupole contribution from the dipole one by studying angular dependence of the pre-edge feature.^{13,14} In particular, in cuprates, only the $3d_{x^2-y^2}$ state is involved in

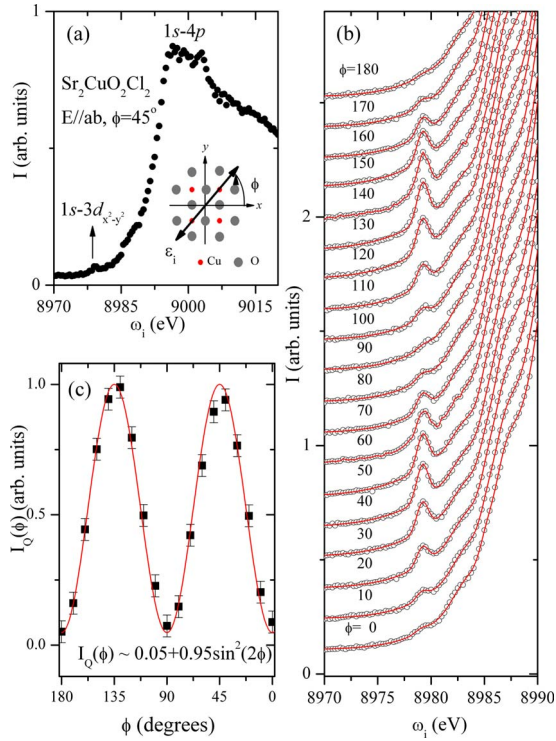


FIG. 1. (Color online) (a) Cu K -edge XAS spectrum of $\text{Sr}_2\text{CuO}_2\text{Cl}_2$. The spectrum shown here is obtained with $\phi=45^\circ$ as shown in the inset. (b) ϕ dependence of the pre-edge region XAS. (c) The pre-edge peak intensity $I(\phi)$ as a function of ϕ . $I(\phi)$ is normalized to have a maximum value of 1. The solid line is $0.05+0.95\sin^2(2\phi)$.

the E2 transition and consequently the quadrupole contribution to the absorption cross-section shows fourfold symmetry. The inset of Fig. 1(a) shows the angle ϕ between the Cu-O bond and the incident photon polarization. The absorption is maximal when the photon polarization is bisecting the Cu-O bond ($\phi=45^\circ$). This observation is consistent with earlier reports on a CuCl_4^{2-} complex¹³ and $\text{Bi}_2\text{Sr}_2\text{CaCu}_2\text{O}_{8+\delta}$.¹⁵ Note that the absorption features due to dipole transitions do not exhibit polarization dependence within the copper-oxygen plane. Detailed ϕ dependence of the pre-edge region is shown in Fig. 1(b). For a quantitative analysis, each spectrum is fitted by a Gaussian function (solid line) and the resulting pre-edge peak intensity, $I(\phi)$, is plotted in Fig. 1(c). The observed fourfold symmetry indicates that the $1s \rightarrow 3d_{x^2-y^2}$ E2 transition contributes dominantly to the pre-edge absorption feature. The sinusoidal dependence $I(\phi) = 0.05 + 0.95 \sin^2(2\phi)$ shown as a solid line in Fig. 1(c) suggests that the E2 contribution is about 95% of the total absorption processes.

By tuning the incident energy at $\omega_i=8979$ eV and $\phi=45^\circ$, we can use the $1s-3d$ intermediate state in our RIXS experiment. With this fixed incident energy and polarization, the scattered photon energy (ω_s) was scanned to obtain RIXS spectra as a function of energy transfer ($\omega \equiv \omega_i - \omega_s$). As shown in Fig. 2(a), a broad peak around $\omega=2$ eV is observed. To demonstrate that this resonance feature is related to the quadrupole intermediate state, we show two separate spectra in the off-resonance condition in which the quadru-

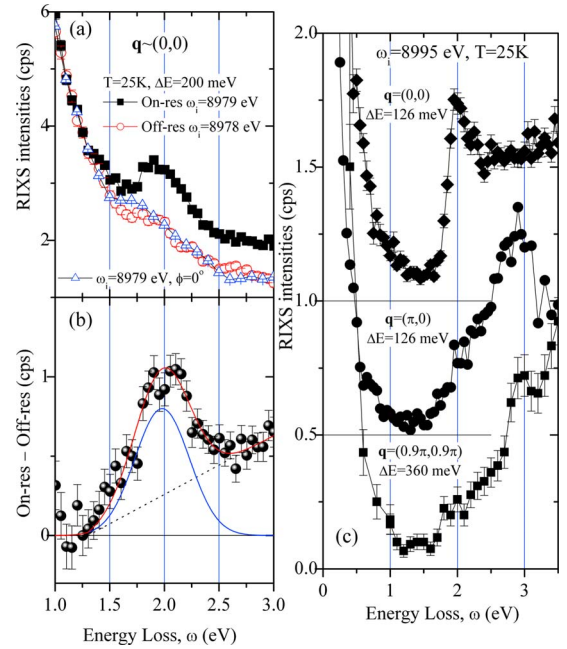


FIG. 2. (Color online) (a) RIXS spectra near $\mathbf{Q} \sim (0, 0, 6.6)$ obtained with the incident photon energy of $\omega_i=8979$ eV and $\phi=45^\circ$. This is compared with spectra obtained with two independent off-resonance conditions: $\omega_i=8978$ eV, $\phi=45^\circ$ and $\omega_i=8979$ eV, $\phi=0^\circ$. (b) Difference curve between on- and off-resonances. The 2 eV feature is fitted by a Gaussian peak with linear background. (c) RIXS spectra at the $1s-4p$ resonance ($\omega_i=8995$ eV) at $\mathbf{q} \sim (0, 0)$, $(\pi, 0)$, and $(0.9\pi, 0.9\pi)$.

pole absorption disappears: changing the incident energy or the incident polarization. The former is $\phi=45^\circ$ and $\omega_i=8978$ eV and the latter $\phi=0^\circ$ and $\omega_i=8979$ eV. As shown in Fig. 2(a), these off-resonance RIXS spectra confirm that the resonantly enhanced feature around 2 eV is due to the intermediate state accessed through the quadrupole absorption. The difference between the on- and off-resonance data obtained with higher resolution is shown in Fig. 2(b). In addition to a well-defined Gaussian peak, gradual increase of the spectral intensity at higher energy is observed, which could be due to the CT excitation.

In Fig. 2(c), we show $1s-4p$ RIXS spectra obtained by choosing the incident energy coinciding with the main absorption peak ($\omega_i=8995$ eV). In a similar monolayer compound La_2CuO_4 , $\mathbf{q}=(0, 0)$ RIXS spectrum shows a strong 2 eV peak, which corresponds to a spin-singlet bound exciton of CT origin.^{8,16-18} In addition to the 2 eV peak, a shoulder peak at lower energy ~ 1.7 eV was observed in La_2CuO_4 and assigned to a $d-d$ excitation.⁸ For finite momentum transfer, the 2 eV CT exciton peak disperses to higher energy while the $d-d$ excitation remains dispersionless. The $1s-4p$ spectra in Fig. 2(c) are very similar to those observed for La_2CuO_4 . That is, a sharp ~ 2 eV peak is observed at $\mathbf{q}=(0, 0)$, which disperses to higher energy at larger \mathbf{q} , while a dispersionless shoulder feature around 2 eV remains at $\mathbf{q}=(\pi, \pi)$ and $(\pi, 0)$ when the CT peak moves away to higher energy. The only difference is that the $d-d$ excitation energy in $\text{Sr}_2\text{CuO}_2\text{Cl}_2$ is around 2 eV instead of 1.7 eV. This supports our assignment of the 2 eV peak in $\text{Sr}_2\text{CuO}_2\text{Cl}_2$ as a

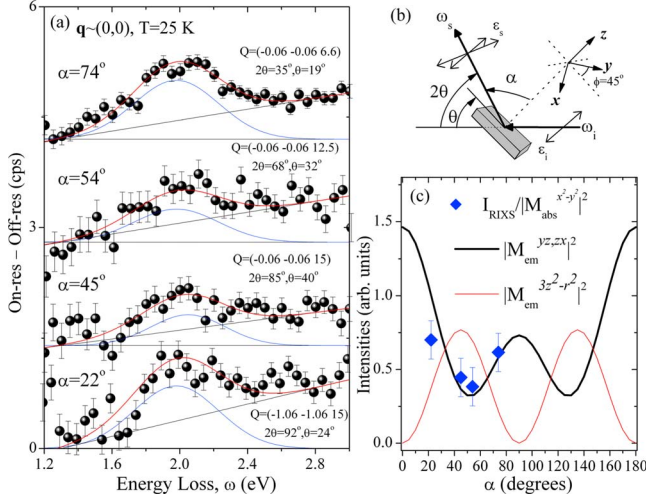


FIG. 3. (Color online) (a) Off-resonance data subtracted RIXS spectra ($\phi=45^\circ$) near $\mathbf{q}\sim(0,0)$. From top to bottom, scattered angle relative to the sample surface normal (α) decreases indicating more sample normal scattering. (b) Schematic of the measurement geometry and angles. (c) The RIXS intensity normalized by $|M_{abs}^{x^2-y^2}|^2$ is plotted as a function of angle α . The angular dependence of the calculated $|M_{em}^{yz,zx}|^2$ and $|M_{em}^{3z^2-r^2}|^2$ is also shown in an arbitrary scale.

$d-d$ excitation, which is further corroborated by the scattering angle dependence of the RIXS matrix element as shown below.

In Fig. 3(a), angle dependence of the 2 eV feature is displayed as a function of scattered angle α , which is the angle between the sample surface normal and the scattered wave vector as shown in Fig. 3(b). The details of measurement geometry are also shown in Fig. 3(b): x , y , and z refer to the sample coordinates, with $x(y)$ and z along the Cu-O bond and the c direction, respectively. Each spectrum is normalized using the $K\beta_5$ emission intensity in order to account for self-absorption. The intensity of the 2 eV feature exhibits non-monotonic α dependence as shown in Fig. 3(a); that is, the intensity is small when $\alpha=54^\circ$ and 45° , while the intensity grows when $\alpha=74^\circ$ and 22° . The 2 eV feature is fitted by a Gaussian function of FWHM=500 meV centered at $\omega\approx 2$ eV with a sloping background for the high-energy spectral weight as shown in Fig. 2(b). Figure 3(c) shows the resultant intensity data normalized by the incident absorption cross-section, which will be discussed below. As mentioned above, the 2 eV feature intensity is small in the vicinity of $\alpha=45^\circ$.

To understand the α dependence of the 2 eV feature, we have calculated RIXS cross-section based on the Kramers-Heisenberg formula

$$I \propto \sum_f \left| \sum_m \frac{M_{em} M_{abs}}{E_m - E_g - \hbar\omega_i - i\Gamma_m} \right|^2, \quad (1)$$

where the matrix elements are $M_{abs}=\langle m|T|g\rangle$ and $M_{em}=\langle f|T|m\rangle$, and $|g\rangle$, $|m\rangle$, and $|f\rangle$ denote the ground, intermediate, and final states of the system, respectively. Note that T is the E2 transition operator here instead of usual

TABLE I. Comparison of the $d-d$ excitations in $\text{Sr}_2\text{CuO}_2\text{Cl}_2$ reported using various experimental methods. THG is third harmonic generation and $\sigma(\omega)$ is the real part of optical conductivity.

Method	Energy (eV)	Symmetry	Reference
RIXS (Cu M)	1.35	xy	3
	1.7	xz^a	
RIXS (Cu L)	1.3–1.5 ^b	$xy+xz$	4
RIXS (O K)	2	$xy+xz$	20
$\sigma(\omega)$	1.5		21
THG	2	$3z^2-r^2$	2
Raman ^c	1.7	xy	1
RIXS (Cu K)	2	xz	This work

^a xz and yz are degenerate in tetragonal $\text{Sr}_2\text{CuO}_2\text{Cl}_2$.

^bZero-energy-loss offset problem.

^c La_2CuO_4 .

dipole one. In the intermediate state, $1s$ core electron is excited to fill the $3d_{x^2-y^2}$ hole: $M_{abs}=\langle 1s|T|3d_{x^2-y^2}\rangle$. In the $d-d$ excitation final state, the $1s$ core hole is filled by electrons from the other d states. Since $\langle 3d_{xy}|T|1s\rangle$ is zero for $\phi=45^\circ$,¹⁹ the matrix elements are nonzero only for the electrons in $3d_{yz,zx}$ or $3d_{3z^2-r^2}$ states: $M_{em}^\eta \equiv \langle 3d_\eta|T|1s\rangle$, where $\eta=yz, zx$ or $3z^2-r^2$. The RIXS intensity is then proportional to overall matrix element given by the product $|M_{abs}^{x^2-y^2}|^2|M_{em}^\eta|^2$. The transition probabilities (M_{abs} and M_{em}) have been calculated using the simple analytical formulas given in Ref. 14 for the symmetry groups D_{4h} ($4/mmm$) based on a spherical tensor expansion of the cross-section.

In Fig. 3(c), calculated results for $|M_{em}^{yz,zx}|^2$ and $|M_{em}^{3z^2-r^2}|^2$ are plotted and compared with experimental data. Since $|M_{abs}^{x^2-y^2}|^2$ is proportional to $\cos^2(\theta)$ according to Ref. 14, where θ is the angle between the wave vector and the sample surface as shown in Fig. 3(b), the experimental data normalized with the $|M_{abs}^{x^2-y^2}|^2$ factor are plotted in Fig. 3(c). $|M_{em}^{yz,zx}|^2$ is at local maxima at $\alpha=0^\circ$ and 90° and local minimum at $\alpha\sim 50^\circ$. Considering uncertainties due to absorption correction and the background subtraction, the agreement between the experimental data and the calculated $|M_{em}^{yz,zx}|^2$ is reasonable. On the other hand, the opposite behavior is expected for $|M_{em}^{3z^2-r^2}|^2$ with maximum at $\alpha=45^\circ$. Therefore most of the spectral weight of the 2 eV peak is likely due to the $d_{x^2-y^2}$ to $d_{yz,zx}$ excitation.

One of the main difficulties in analyzing the observed spectra is the broad linewidth, which is much broader than the instrumental resolution [e.g., see Fig. 2(b)]. This is presumably due to the presence of multiple $d-d$ excitations within narrow energy range of 1.5–2.5 eV. In Table I, $d-d$ excitation energies measured with various spectroscopic techniques for $\text{Sr}_2\text{CuO}_2\text{Cl}_2$ are listed. Cu $M_{2,3}$ -edge,³ L_3 -edge,⁴ and O K -edge²⁰ studies, it was shown that $d_{yz,zx}$ is the highest $d-d$ excitation. While former two studies establish 1.7 eV as its energy, the O K -edge study assigns a peak at 2 eV to the $d_{yz,zx}$ excitation.²² We note that $d-d$ excitation feature of La_2CuO_4 is located at around 2 eV in the recent

L_3 -edge RIXS paper²³ but 1.7 eV in Ref. 4, because zero-energy calibration is uncertain due to the small elastic intensity and the existence of two magnon peak at 0.3–0.4 eV. Considering that two magnon also exists in $\text{Sr}_2\text{CuO}_2\text{Cl}_2$, it is most plausible that the correct $d_{yz,zx}$ excitation energy is higher than 1.7 eV which is estimated in the previous L_3 -edge study of Ref. 4. We believe that the zero-energy calibration is more accurate in the case of Cu K -edge RIXS due to a prominent elastic intensity and a high resolution. Other d - d excitations, d_{xy} and $d_{3z^2-r^2}$, are expected at lower energy. But the $M_{2,3}$ edge and L_3 edge do not agree with each other on these two d - d excitations; the lowest is d_{xy} in the $M_{2,3}$ -edge study but $d_{3z^2-r^2}$ in the L_3 -edge study. The $d_{3z^2-r^2}$ excitation, in principle, can be probed and distinguished from the $d_{yz,zx}$ by an angular dependence in the quadrupole RIXS. In the current work, we cannot identify $d_{3z^2-r^2}$. This might be due to a small intensity obscured by $|M_{em}^{yz,zx}|^2$ and the elastic tail. It will be an interesting future work to probe $d_{3z^2-r^2}$ using the horizontal scattering geometry (π -incident polarization) with higher energy resolution.

In summary, we find that the in-plane pre-edge peak of $\text{Sr}_2\text{CuO}_2\text{Cl}_2$ mostly consists of the $1g$ - $3d_{x^2-y^2}$ electric quadrupole transition through the fourfold azimuthal angle dependence of the pre-edge peak. Using the quadrupole resonance, we observed a RIXS excitation at 2 eV energy loss. We find that the polarization dependence of the 2 eV excitation is consistent with the $d_{x^2-y^2}$ to $d_{yz,zx}$ excitation. This study demonstrates the important role of the electric quadrupole transition and the utility of the Cu K pre-edge RIXS as a symmetry-sensitive probe of orbital excitation in cuprates.

The work at University of Toronto was supported by Natural Sciences and Engineering Research Council of Canada and by Ontario Ministry of Research and Innovation through Early Researcher Award. Use of the Advanced Photon Source was supported by the U.S. DOE, Office of Science, Office of Basic Energy Sciences, under Contract No. W-31-109-ENG-38.

*yjkim@physics.utoronto.ca

- ¹D. Salamon, R. Liu, M. V. Klein, M. A. Karlow, S. L. Cooper, S. W. Cheong, W. C. Lee, and D. M. Ginsberg, Phys. Rev. B **51**, 6617 (1995).
- ²A. B. Schumacher, J. S. Dodge, M. A. Carnahan, R. A. Kaindl, D. S. Chemla, and L. L. Miller, Phys. Rev. Lett. **87**, 127006 (2001).
- ³P. Kuiper, J.-H. Guo, C. Sathe, L.-C. Duda, J. Nordgren, J. J. M. Poethuizen, F. M. F. de Groot, and G. A. Sawatzky, Phys. Rev. Lett. **80**, 5204 (1998).
- ⁴G. Ghiringhelli, N. B. Brookes, E. Annese, H. Berger, C. Dallera, M. Grioni, L. Perfetti, A. Tagliaferri, and L. Braicovich, Phys. Rev. Lett. **92**, 117406 (2004).
- ⁵Y. J. Kim, J. P. Hill, F. C. Chou, D. Casa, T. Gog, and C. T. Venkataraman, Phys. Rev. B **69**, 155105 (2004).
- ⁶S. Suga, S. Imada, A. Higashiya, A. Shigemoto, S. Kasai, M. Sing, H. Fujiwara, A. Sekiyama, A. Yamasaki, C. Kim, T. Nomura, J. Igarashi, M. Yabashi, and T. Ishikawa, Phys. Rev. B **72**, 081101(R) (2005).
- ⁷J. W. Seo, K. Yang, D. W. Lee, Y. S. Roh, J. H. Kim, H. Eisaki, H. Ishii, I. Jarrige, Y. Q. Cai, D. L. Feng, *et al.*, Phys. Rev. B **73**, 161104(R) (2006).
- ⁸D. S. Ellis, J. P. Hill, S. Wakimoto, R. J. Birgeneau, D. Casa, T. Gog, and Y.-J. Kim, Phys. Rev. B **77**, 060501(R) (2008).
- ⁹A. Kotani and S. Shin, Rev. Mod. Phys. **73**, 203 (2001).
- ¹⁰B. C. Larson, J. Z. Tischler, W. Ku, C.-C. Lee, O. D. Restrepo, A. G. Eguiluz, P. Zschack, and K. D. Finkelstein, Phys. Rev. Lett. **99**, 026401 (2007).
- ¹¹S. Huotari, T. Pylkkanen, G. Vanko, R. Verbeni, P. Glatzel, and G. Monaco, Phys. Rev. B **78**, 041102(R) (2008).
- ¹²L. L. Miller, X. L. Wang, S. X. Wang, C. Stassis, D. C. Johnston, J. J. Faber, and C.-K. Loong, Phys. Rev. B **41**, 1921 (1990).
- ¹³J. E. Hahn, R. A. Scott, K. O. Hodgson, S. Doniach, S. R. Desjardins, and E. I. Solomon, Chem. Phys. Lett. **88**, 595 (1982).
- ¹⁴C. Brouder, J. Phys.: Condens. Matter **2**, 701 (1990).
- ¹⁵N. L. Saini, A. Lanzara, A. Bianconi, and H. Oyanagi, Phys. Rev. B **58**, 11768 (1998).
- ¹⁶Y. J. Kim, J. P. Hill, C. A. Burns, S. Wakimoto, R. J. Birgeneau, D. Casa, T. Gog, and C. T. Venkataraman, Phys. Rev. Lett. **89**, 177003 (2002).
- ¹⁷E. Collart, A. Shukla, J.-P. Rueff, P. Leininger, H. Ishii, I. Jarrige, Y. Q. Cai, S.-W. Cheong, and G. Dhalenne, Phys. Rev. Lett. **96**, 157004 (2006).
- ¹⁸L. Lu, J. N. Hancock, G. Chabot-Couture, K. Ishii, O. P. Vajk, G. Yu, J. Mizuki, D. Casa, T. Gog, and M. Greven, Phys. Rev. B **74**, 224509 (2006).
- ¹⁹Scattered photon polarization cannot be analyzed currently, and we assume that the emitted photon is still linearly polarized along the incident polarization.
- ²⁰Y. Harada, K. Okada, R. Eguchi, A. Kotani, H. Takagi, T. Takeuchi, and S. Shin, Phys. Rev. B **66**, 165104 (2002).
- ²¹H. S. Choi, Y. S. Lee, T. W. Noh, E. J. Choi, Y. Bang, and Y. J. Kim, Phys. Rev. B **60**, 4646 (1999).
- ²²Only final hole state is referred in the rest of the discussion with the understanding that the initial hole is in $d_{x^2-y^2}$.
- ²³L. Braicovich, L. J. P. Ament, V. Bisogni, F. Forte, C. Aruta, G. Balestrino, N. B. Brookes, G. M. D. Luca, P. G. Medaglia, F. M. Granozio *et al.*, Phys. Rev. Lett. **102**, 167401 (2009).